Chemical Physics Letters 733 (2019) 136693

Contents lists available at ScienceDirect

Chemical Physics Letters

journal homepage: www.elsevier.com/locate/cplett

Research paper

Seventeen-coordinate binary metal superatoms: M@Li_{17}

Lijuan Yan[a], Jianmei Shao[a], Liren Liu[b,*], Chunlei Chen[a,*]

[a] College of Electronics & Information Engineering, Guangdong Ocean University, Zhanjiang 524088, China
[b] State Key Laboratory of Mechanics and Control of Mechanical Structures, Key Laboratory for Intelligent Nano Materials and Devices of Ministry of Education, and Institute of Nanoscience, Nanjing University of Aeronautics and Astronautics, Nanjing 210016, China

HIGHLIGHTS

- A series of seventeen-coordinate metal clusters M@Li_{17} (M = Ca, Sr, Ba, Sc, Y) have been identified.
- M@Li_{17} (M = Sc, Y), is highly stable, nonmagnetic, and a large HOMO-LUMO gap.
- M@Li_{17} (M = Ca, Sr, Ba), is highly stable, but a low spin magnetic moment of 1 μ_B and a small HOMO-LUMO gap.

ARTICLE INFO

Keywords:
High coordination
Superatoms
Stability
Energy gap
Magnetic moment

ABSTRACT

Stable metal clusters with high coordination numbers (N > 12) are scarce. In this paper, series of seventeen-coordinate metal clusters M@Li_{17} (M = Ca, Sr, Ba, Sc, Y) are proposed, where the lithium atoms compose the outer cage and the hetero-atom is centered. The unique structure is located as a low energy isomer by particle swarm optimisation algorithm. With the geometric and electronic shell closures, the high stability of M@Li_{17} (M = Sc, Y) is predictable. For the 19-electron M@Li_{17} (M = Ca, Sr, Ba), the electronic configurations are $1S^21P^61D^{10}2S_\alpha^{\ 1}2S_\beta^{\ 0}$, which can obtain their stability by forming a low magnetic moment of 1 μ_B.

1. Introduction

One of the interesting issues in cluster science is to design stable clusters, important for both basic research and applications. Among them, superatoms, also regarded as the ideal building units for cluster assembled materials, are most appealing clusters due to their high stability and the ability of tuned properties through selection of size, composition and charge state [1–3]. For example, the centred icosahedral Al_{13}^- cluster is a typical superatom known for its pronounced stability, which could mimic the chemical behaviour of inert gas atoms in the periodic table. With one electron taken out, the properties of 39-electron Al_{13} cluster are analogous to a halogen atom [4]. While the central aluminum atom is replaced by other elements, such as Cu, P, C or Si, the icosahedral geometric structure remains still with the properties resembled to a phosphorus, an alkali superatom, or a noble gas superatom, respectively [5–9]. The similar situation occurs in M@B_n [10], M@Si_n [11–13], and M@Sn_n [14] by the variation of the endohedral metal atom. In addition, researches show that the stability of a cluster is enhanced by its electronic and geometric shell closures [15].

For the metal clusters, their electronic shells can be explained by the jellium model, where the motions of valence electrons are subjected in an assumed uniform positive spherical potential composed by the atomic nuclei and the innermost electrons of the clusters [16,17]. The valence electronic filling orders in the metal clusters are $1S^21P^61D^{10}2S^21F^{14}2P^61G^{18}$..., with S, P, D, F, G, etc., denoting the angular momenta. The numbers of valence electrons 2, 8, 18, 20, 34, 40, 58, etc. correspond to the closed electronic shell. Therefore, the high stability of Al_{13}^-, of which the 40 valence electrons arise from three valence electrons offered by each aluminum atom and the addition of a negative charge, is due to its closed geometric and electronic shells. With all the electrons paired, Al_{13}^- is identified as a non-magnetic superatom. In 2009, Khanna and coworkers extended the concept of the superatom to unpaired species [18], which were composite systems with relatively localized orbitals and diffuse valence orbitals to offer their magnetic moments and stability, respectively. As an example, an isolated VCs_8 and a ligated protected $MnAu_{24}(SH)_{18}$ clusters are design to demonstrate the intriguing possibility, both of them with a magnetic moment of 5μ_B. Since then, many researches on magnetic superatoms are emerged [19–24].

However, most of superatoms with high coordination numbers (N > 12) are formed by covalent bonds, such as, the metal (M)-encapsulating binary systems M@Si_{16} [11–13], M@Sn_{17} [14] and M@C_{28}

* Corresponding authors.
E-mail addresses: lrliu@nuaa.edu.cn (L. Liu), ccl-cc@163.com (C. Chen).

https://doi.org/10.1016/j.cplett.2019.136693
Received 1 July 2019; Received in revised form 9 August 2019; Accepted 15 August 2019
Available online 16 August 2019

[25], where the core atom handles 16, 17 and 28 outer atoms, respectively. For metal clusters, they are prone to form compact structures and with small coordination, for example, 8-coordinate VNa_8 [18,23], $TMCa_8$ (TM = Sc, Ti, V, Cr, Mn, Fe, Co, …) [20], 9-coordinate $MnSr_9$ [21], 12-coordinate Al_{13} with the endohedral atom either Al or other elements [4–9], $Sc@Na_{12}$ [19], $M@Au_{12}$ [26], 13-coordinate VLi_{13} [22], 14-coordinate $TM@Li_{14}$ (TM = Sc, Ti, V, Y, Zr, Nb, Hf, Ta and W) [24], 16-coordinate $M@Li_{16}$ (M = Ca, Sr, Ba, Ti, Zr, Hf) [27], etc. It is an interesting and challenging task to seek metal superatoms with high coordination, which are deficient at the moment.

In this paper, lithium is selected as a prototype for its lightness and simple electronic shell ($1s^22s^1$), and thus the geometric and electronic structures of lithium clusters are very little affected by relativistic effects, being a good starting for research. On the basis of particle swarm optimisation algorithm (PSO) search and density functional theory (DFT) calculations, series of C_{4v} symmetry 17-coordinate clusters $M@Li_{17}$ (M = Ca, Sr, Ba, Sc, Y) are proposed, where the outer shell is composed by the seventeen lithium atoms and the assigned metal atom is located at the central of the Li_{17} cage. In the following, the stability of $M@Li_{17}$ (M = Ca, Sr, Ba, Sc, Y) are analyzed from the aspects of energy calculations, HOMO–LUMO gaps, geometric structures, and electronic shells, etc.

2. Computational method

The low energy isomers of $M@Li_{17}$ (M = Ca, Sr, Ba, Sc, Y) are searched using the PSO algorithm implemented in Crystal structure AnaLYsis by Particle Swarm Optimization (CALYPSO) package [28]. The structural evolution through PSO algorithm is performed with each generation containing 50 structures, and also the number of generation is set as 50. To guarantee the structural diversity, the 60% best structures generated by PSO algorithm are passed to the next generation and the rest of 40% are new and generated randomly. DistanceOfIon employs the average interatomic distances obtained by experiment or their fine-tuned values for each search with a new initial structure. A vacuum distance of 20 Å is chosen to avoid interactions between images. Then, the located low energy isomers are re-optimized without any symmetry constraint at the DFT levels of Gaussian 16 code [29], and there are no virtual values for frequency calculations confirming that they are true local minima. To yield the most reliable results, three functionals proved valid for the lithium clusters system, namely, pure functional PW91 [30], meta-GGA functional M06-L [31], and hybrid functional TPSSH [32], are adopted. Yet, we select the results of functional PW91 presented in the paper for it is reported in best agreement with the experimental values in the aspects of the bond length, the average binding energy, and the ionization potential [22]. Effective core potentials including relativistic effects are employed on all the metal atoms, and here is the Stuttgart-Dresden ECP (SDD) [33]. Further, the spin multiplicities (SMs) for each isomer are determined by comparing their total energy with the same structures and different SMs, where the SMs of ground states are according to the isomers with the lowest energy. All the pictures are completed by using Multiwfn_3.6.

3. Results and discussion

The seventeen-coordinate binary metal superatoms are assumed for putting an impure atom (M = Ca, Sr, Ba, Sc, Y) into the center of Li_{17} cage. By the search of CALYPSO structure prediction code, the designed cage-like structure is located as a low energy isomer shown in Fig. 1, where only the first six low energy structures are displayed. Due to the high mobility of lithium atoms, the other low energy isomers are prone to change into the present structures in the processes of re-optimization. The lowest energy structures for the $M@Li_{17}$ clusters are all with the C_{4v} symmetry (isomer A) except for $Sc@Li_{17}$ with the C_{2v} symmetry (isomer C), of which the total energy is 0.01 eV lower than that of isomer A at the calculations of PW91/SDD as summarized in Table 1.

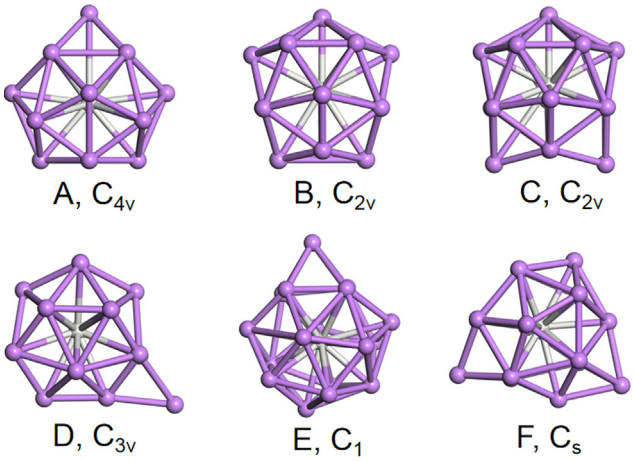

Fig. 1. The first six low energy isomers of $M@Li_{17}$. The white atom is Ca, Sr, Ba, Sc, Y; others are lithium. A: the C_{4v} symmetry spherical shell with a center hetero atom. B: the outer lithium cage with C_{2v} symmetry. C: another C_{2v} symmetry structure with elongated bond lengths of Li-Li at the bottom. D: a lithium atom topped on the C_3 axis of the tetrahedral outer shell. E: one lithium atom is on the surface, the hetero metal atom atom is at the center. F: two lithium atoms are on the C_s symmetry surface.

Table 1
Relative energies (PW91/SDD) of $M@Li_{17}$ (M = Ca, Sr, Ba, Sc, Y) clusters, where the referenced energies with 0.00 eV are their own lowest-energy isomers and the letters A to F correspond to the first six low energy isomers presented in Fig. 1.

M	A	B	C	D	E	F
Sc	0.01	C	0	0.06	0.07	0.08
Y	0	A	0.03	0.08	C	A
Ca	0	0.02	0.03	0.18	C	A
Sr	0	0.01	0.03	0.21	A	A
Ba	0	0.01	0.03	0.18	A	A

The symmetries of outer cages cause their structural differences. Taking $Ca@Li_{17}$ as an example, the C_{4v} symmetry isomer A and the C_{2v} symmetry isomers B and C are with the lengths of Li—Li bond of 2.89–3.35 Å, 2.92–3.41 Å, and 2.88–3.59 Å, respectively, where the energies are successively increased with their structures elongated. However, the corresponding bond lengths of Ca-Li are all at the range 3.28–3.54 Å for the three isomer. Further optimizing these low energy isomers with the parameters gdiis, calcfc, calcall, etc., which are good choices for passing through the potential energy surfaces, the finally structures have the tendency to be the lowest energy structure, further predicting the high stability of the C_{4v} symmetry $M@Li_{17}$ clusters (except for $Sc@Li_{17}$). However, the endohedral doped other transition-metal atoms in the central of Li_{17} cage are inappropriate on account of the mismatch of atomic radius or redundant electron, and thus are not further discussed here.

The stability of C_{4v} symmetry $M@Li_{17}$ (M = Ca, Sr, Ba, Sc, and Y) clusters are further confirmed by the average binding energy (E_b) per atom, which is defined as the energy difference between the total energy of all the free atoms and the total energy of complexes formulized as:

$$E_b(M@Li_{17}) = \frac{E(M) + 17E(Li) - E(M@Li_{17})}{18}$$

The fragmentation energy (E_f), which denotes the gain in binding energy by successively adding a Li atom to the preceding size $M@Li_{n-1}$ cluster, also can be used to describe the degree of dissociation obtained from the following equation:

$$E_f(M@Li_{17}) = E(M@Li_{16}) + E(Li) - E(M@Li_{17})$$

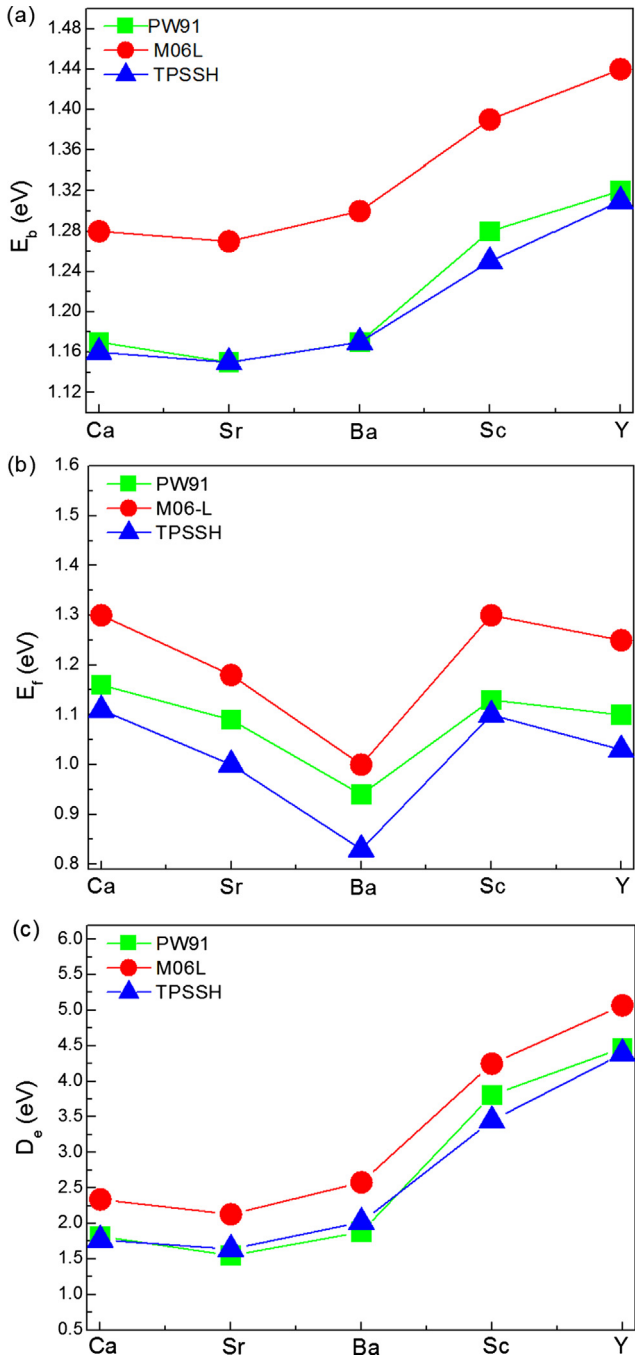

Fig. 2. The (a) average binding energy (E_b) per atom, (b) fragmentation energy (E_f), and (c) embedding energy (D_e) of the C_{4v} symmetry M@Li_{17} (M = Ca, Sr, Ba, Sc, and Y) clusters.

For endohedral cage-like clusters, we also calculate their embedding energy (D_e) to evaluate the possibility of embedding an atom in the central of outer cage, i.e. the interaction between the outer shell and an embedded atom. Generally, D_e is defined as:

$$D_e(M@Li_{17}) = E(shell) + E(core) - E(M@Li_{17})$$

In the above three formulas, M represents the embedded elements Ca, Sr, Ba, Sc, and Y. E(M@Li_{17}) and E(M@Li_{16}) denote the total energy of the C_{4v} symmetry M@Li_{17} clusters and that of their fragments M@Li_{16} formed by one lithium detached from M@Li_{17}. E(shell) and E(core) represent the total energies of the outer shell and the central elements, respectively. E(Li) and E(M) are the total energy of Li element and endohedral elements in their free states, respectively.

Fig. 2 gives the diagrams of the above calculated results. The average binding energies per atom of M@Li_{17} (M = Ca, Sr, Ba) is almost alike, which can be significantly enhanced by replacing the endohedral atom with the transition-metal elements Sc or Y. Comparing with the same main group as the core, the fragmentation energy of M@Li_{17} (M = Ca, Sr, Ba, Sc, and Y) is decreasing monotonically with the increasing electron counts, and thus the dissociation is easier. All the values of D_e are positive, which verify the feasibilities that the chosen elements (M = Ca, Sr, Ba, Sc, and Y) can be encapsulated into Li_{17} cage. The relative large D_e values of M@Li_{17} (M = Sc, Y) indicate Sc or Y are more suitable to embed into Li_{17} cage forming stable seventeen-coordinate clusters.

The HOMO-LUMO gaps (the energy difference of highest occupied molecular orbital and lowest unoccupied molecular orbital) are also calculated to examine the stability of C_{4v} symmetry M@Li_{17} (M = Ca, Sr, Ba, Sc, Y) clusters. A large HOMO–LUMO gap will enhance the stability. For the 20-electron Sc@Li_{17} and Y@Li_{17} clusters, their gaps are 0.83 and 0.72 eV, respectively, at PW91/SDD level, while the values of M@Li_{17} (M = Ca, Sr, Ba) are all 0.19 eV. Comparing to the gaps of typical superatoms, such as the metal superatom Al_{13}^- (1.87 eV) [34] and the covalently bonded C_{60} (1.72 eV) [35], the gaps of Sc@Li_{17} and Y@Li_{17} are moderate, but that of M@Li_{17} (M = Ca, Sr, Ba) seems too small. However, from the view of magnetic superatoms their gaps can be compared, for example, V@Na_8 (0.69 eV) [18,23], $MnSr_9$ (0.35 eV) [21], Pb@Mn_{12}@Pb_{20} (0.38 eV) [36], etc. Moreover, the energy gaps often are underestimated by the standard GGA functionals, and thus we give more accurate values by using the hybrid functional TPSSH shown in Fig. 3.

The moderate HOMO–LUMO gaps of M@Li_{17} (M = Sc, and Y) clusters indicate that they are with relative high stability, where the gaps of M@Li_{17} (M = Ca, Sr, Ba) are a little small but rational for magnetic superatoms. In the following, we analyze the microscopic mechanism of their stability from the points of electronic shells. 19-electron Ca@Li_{17} and 20-electron Y@Li_{17} are chosen as representative clusters for the properties of M@Li_{17} (M = Sr, Ba, Sc) can be analogized due to with the same effective valence electrons.

For Ca@Li_{17}, its one electron energy levels and molecular orbitals (MOs) are shown in Fig. 4(a), and the characters of the orbitals are identified by comparing the global shape and nodes with atomic orbitals. The lowest state has 1S character due to the MO over the whole cluster. The next three states are with the character of 1P, where the $1P_z$ is about 0.09 eV higher in energy than the $1P_x$, $1P_y$ states at the calculations of PW91/SDD. The occurrence is caused by the oblate shape of the cluster. Also, the next five 1D orbitals have been split into four groups with 1, 1, 1, and 2 orbitals, respectively. The last occupied state is also spread out over the whole cluster and identified with 2S

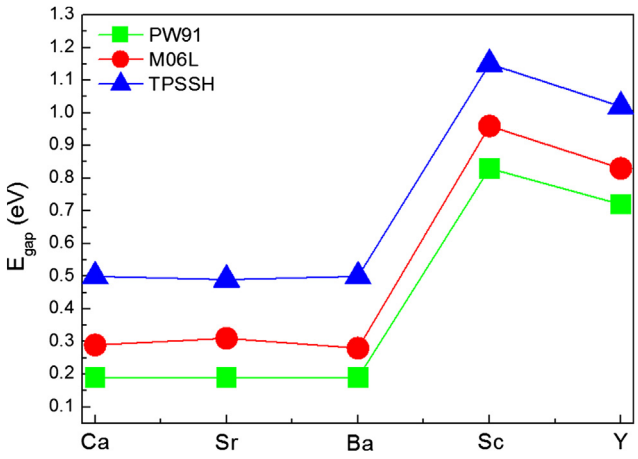

Fig. 3. Variation of HOMO–LUMO energy gap (E_{gap}) with the M atom for M@Li_{17} clusters.

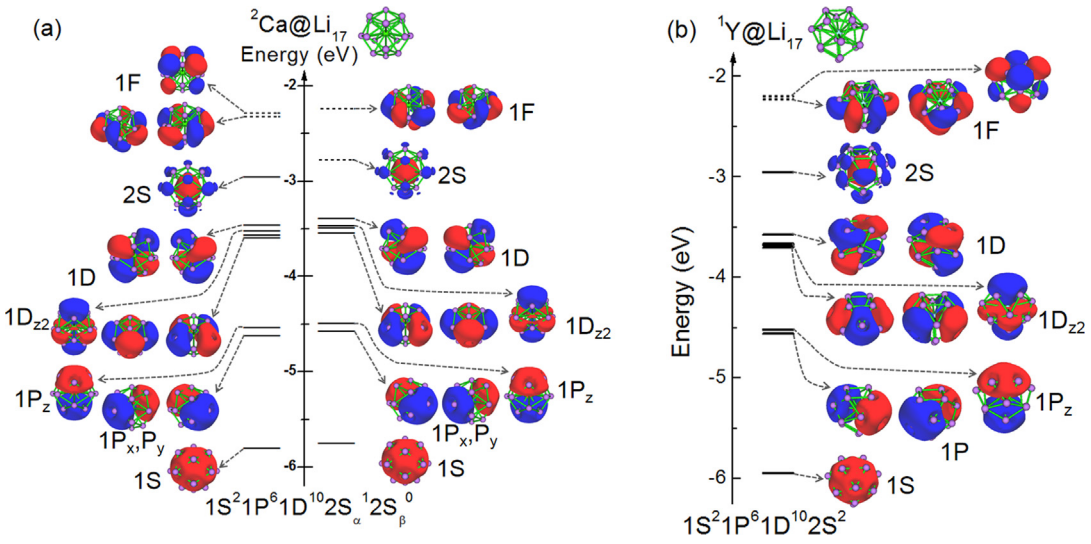

Fig. 4. One electron energy levels and molecular orbitals of Ca@Li_{17} (a) and Y@Li_{17} (b).

character. Resembling to the discussion of previous work [37–39], the origin of the 2S shell in the spherical symmetry Ca@Li_{17} cluster is the antibonding combination between the 4s and 1s shells of the endohedral Ca atom and [Li_{17}]. Corresponding, the electronic configuration of Ca@Li_{17} is $1S^21P^61D^{10}2S_\alpha{}^12S_\beta{}^0$. Its formation mainly involves the interaction between the s- and d-type shells of Ca element and the jellium shells of [Li_{17}]. Since Ca@Li_{17} has 19 valence electrons, the remained one electron resides in 2S orbital. With a pure orbital angular momentum l = 0, the spin-orbit coupling will lead to a single total-angular momenta j (j = l + s), i.e. a pure spin angular momentum of 1.0 μ_B. Similarly, the filling order of 20-electron Y@Li_{17} is $1S^21P^61D^{10}2S^2$, which is a non-magnetic cluster due to all the electron paired seen from Fig. 4(b).

Based on above analysis, all of the C_{4v} symmetry M@Li_{17} (M = Ca, Sr, Ba, Sc, Y) clusters can be identified as superatoms. For the 20-electron M@Li_{17} (M = Sc, Y), their stability can be enhanced by the closed geometric structures and electronic shells. Whereas the 19-electron M@Li_{17} (M = Ca, Sr, Ba) with open electronic shells, they can stabilize themselves by forming a low spin magnetic moment of 1 μ_B. In addition, the degeneracy of the 1P and 1D orbitals are split for the flat geometry, where the lengths of Ca-Li are 3.29–3.51 Å for Ca@Li_{17} and that of Y-Li are 3.20–3.44 Å for Y@Li_{17}. The more oblate geometric structure of Ca@Li_{17} leads to the larger splitting of the degenerate 1P and 1D orbitals.

4. Conclusions

To summary, a range of high-coordinate metal clusters M@Li_{17} (M = Ca, Sr, Ba, Sc, Y) are proposed through an unbiased global optimization method (PSO) and DFT calculation, where the designated core atom can hold seventeen lithium atoms. Energy calculations show that the C_{4v} symmetry clusters are very stable. MOs analysis confirms the characters of superatomic molecular orbitals in these high symmetric clusters. Such a combination of Li_{17} cage and a core atom can be expanded in the same main group as the dopants, such as Ca, Sr and Ba. Other high-coordinate metal clusters would be worth further exploration.

Declaration of Competing Interest

The authors declare that they have no competing financial interest.

Acknowledgement

This work is supported by the Special Foundation for Theoretical Physics Research Program of China (no.11847119), by the National Natural Science Foundation of China [no. 11704080, no. 21763024], by the PhD Starting Fund of Guangdong Ocean University [no. 120702/R17077], by the China Postdoctoral Science Foundation (no. 2018M632301).

Appendix A. Supplementary material

Supplementary data to this article can be found online at https://doi.org/10.1016/j.cplett.2019.136693.

References

[1] S.N. Khanna, P. Jena, Phys. Rev. B: Condens. Matter 51 (1995) 13705.
[2] A.W. Castleman Jr., S.N. Khanna, J. Phys. Chem. C 113 (2009) 2664.
[3] S.A. Claridge, A.W. Castleman Jr., S.N. Khanna, C.B. Murray, A. Sen, P.S. Weiss, ACS Nano 3 (2009) 244.
[4] D.E. Bergeron, A.W. Castleman Jr., T. Morisato, S.N. Khanna, Science 304 (2004) 84.
[5] J.U. Reveles, T. Baruah, R.R. Zope, J. Phys. Chem. C 119 (2015) 5129.
[6] S.K. Nayak, S.N. Khanna, P. Jena, Phys. Rev. B 57 (1998).
[7] B. Wang, J. Zhao, D. Shi, X. Chen, G. Wang, Phys. Rev. A 72 (2005).
[8] X.G. Gong, V.V. Kumar, Phys. Rev. Lett. 70 (1993) 2078.
[9] B. Molina, J.R. Soto, J.J. Castro, J. Phys. Chem. C 116 (2012) 9290.
[10] H.J. Zhai, Y.F. Zhao, W.L. Li, Q. Chen, H. Bai, H.S. Hu, Z.A. Piazza, W.J. Tian, H.G. Lu, Y.B. Wu, Y.W. Mu, G.F. Wei, Z.P. Liu, J. Li, S.D. Li, L.S. Wang, Nat Chem 6 (2014) 727.
[11] K. Koyasu, M. Akutsu, M. Mitsui, A. Nakajima, J. Am. Chem. Soc. 127 (2005) 4998.
[12] M. Shibuta, T. Ohta, M. Nakaya, H. Tsunoyama, T. Eguchi, A. Nakajima, J. Am. Chem. Soc. 137 (2015) 14015.
[13] H. Tsunoyama, H. Akatsuka, M. Shibuta, T. Iwasa, Y. Mizuhata, N. Tokitoh, A. Nakajima, J. Phys. Chem. C 121 (2017) 20507.
[14] J. Atobe, K. Koyasu, S. Furuse, A. Nakajima, Phys. Chem. Chem. Phys. 14 (2012) 9403.
[15] A.C. Reber, S.N. Khanna, Acc. Chem. Res. 50 (2017) 255.
[16] W. Ekardt, Phys. Rev. B 29 (1984) 1558.
[17] W. Ekardt, Phys. Rev. B: Condens. Matter 34 (1986) 526.
[18] J.U. Reveles, P.A. Clayborne, A.C. Reber, S.N. Khanna, K. Pradhan, P. Sen, M.R. Pederson, Nat. Chem. 1 (2009) 310.
[19] K. Pradhan, J.U. Reveles, P. Sen, S.N. Khanna, J. Chem. Phys. 132 (2010) 124302.
[20] V. Chauhan, V.M. Medel, J. Ulises Reveles, S.N. Khanna, P. Sen, Chem. Phys. Lett. 528 (2012) 39.
[21] V. Medel, J.U. Reveles, S.N. Khanna, J. Appl. Phys. 112 (2012) 064313.
[22] M. Zhang, J. Zhang, X. Feng, H. Zhang, L. Zhao, Y. Luo, W. Cao, J. Phys. Chem. A 117 (2013) 13025.
[23] X. Zhang, Y. Wang, H. Wang, A. Lim, G. Gantefoer, K.H. Bowen, J.U. Reveles, S.N. Khanna, J. Am. Chem. Soc. 135 (2013) 4856.
[24] L. Yan, J. Liu, J. Shao, Mol. Phys. (2019), https://doi.org/10.1080/00268976.2019.1592256.

[25] J.P. Dognon, C. Clavaguera, P. Pyykko, J. Am. Chem. Soc. 131 (2009) 238.
[26] H.J. Zhai, J. Li, L.S. Wang, J. Chem. Phys. 121 (2004) 8369.
[27] X. Gu, G.H. Chen, M. Ji, Y.X. Yao, X.G. Gong, Nanoscale 4 (2012) 2567.
[28] J. Lv, Y. Wang, L. Zhu, Y. Ma, J. Chem. Phys. 137 (2012) 084104.
[29] M.J. Frisch, G.W. Trucks, H.B. Schlegel, G.E. Scuseria, M.A. Robb, J.R. Cheeseman, G. Scalmani, V. Barone, B. Mennucci, G.A.e. Petersson, Gaussian, Inc.:Wallingford, Ct, 2016.
[30] J.P. Perdew, Y. Wang, Phys. Rev. B: Condens. Matter 45 (1992) 13244.
[31] Y. Zhao, D.G. Truhlar, J. Chem. Phys. 125 (2006) 194101.
[32] S. Grimme, J. Antony, S. Ehrlich, H. Krieg, J. Chem. Phys. 132 (2010) 154104.
[33] T. Lu, F. Chen, J. Comput. Chem. 33 (2012) 580.
[34] S.N. Khanna, B.K. Rao, P. Jena, Phys. Rev. B 65 (2002).
[35] X.G. Gong, Q.Q. Zheng, Phys. Rev. B: Condens. Matter 52 (1995) 4756.
[36] X. Huang, J. Zhao, Y. Su, Z. Chen, R.B. King, Sci. Rep. 4 (2014) 6915.
[37] A. Muñoz-Castro, J. Phys. Chem. Lett. 4 (2013) 3363.
[38] A. Muñoz-Castro, R.B. King, J. Phys. Chem. C 121 (2017) 5848.
[39] F. Gam, R. Arratia-Perez, S. Kahlal, J.-Y. Saillard, A. Muñoz-Castro, J. Phys. Chem. C 122 (2018) 4723.